Journal of Solid State Chemistry 185 (2012) 219–224

Contents lists available at SciVerse ScienceDirect

Journal of Solid State Chemistry

journal homepage: www.elsevier.com/locate/jssc

8-Hydroxypyrene-1,3,6-trisulphonate and octanesulphonate co-assembled layered double hydroxide and its controllable solid-state luminescence by hydrothermal synthesis

Sile Dang, Dongpeng Yan, Jun Lu*

State Key Laboratory of Chemical Resource Engineering, Beijing University of Chemical Technology, Beijing 100029, PR China

ARTICLE INFO

Article history:
Received 27 July 2011
Received in revised form
25 October 2011
Accepted 30 October 2011
Available online 12 November 2011

Keywords:
Dual-color fluorescence
Layered double hydroxide
Hydrothermal synthesis
Intercalation

ABSTRACT

8-Hydroxy-pyrene-1,3,6-trisulphonate (HPTS) and octanesulphonate (OS) have been co-intercalated into the ZnAl layered double hydroxide (LDH) host by a hydrothermal co-precipitation method, with samples denoted as HPTS (x%)-OS/Zn_2Al-LDH (x stands for the molar percentage content of HPTS with respect to total amount of HPTS and OS). The structure and chemical compositions of the as-prepared compounds were characterized by X-ray diffraction (XRD) and elemental analysis. The steady-state and time-decay fluorescent studies show that HPTS (2%)-OS/Zn_2Al-LDH has the optimal luminous emission and the longest fluorescent lifetime. Moreover, these samples exhibit controllable dual fluorescence between the blue and green regions upon changing the interlayer HPTS content, external pH values, and host–guest interaction, illustrating that these organic–inorganic samples have potential application in the field of tunable solid luminescent materials.

1. Introduction

Organic–inorganic hybrid materials have received considerable attention owing to their advantages by combining both the organic and inorganic parts [1]. Layered double hydroxides (LDHs) are a large class of inorganic anionic clays, which can be described by the general formula $[M^{II}_{1-x}M^{III}_x(OH)_2][A^{n-}_{x/n}\cdot mH_2O]$ where M^{II} and M^{III} are divalent and trivalent metals, respectively, and A^{n-} is an anion. The host structure features positively charged hydroxide layers, which are electrically balanced by the intercalation of anions in the interlayer space, and the interlayer anions can also be replaced by other ones to construct a plenty of new functional materials. Recently, fluorescence molecules intercalated LDH have been reported [2–6], and the layered organic–inorganic hybrid materials exhibited excellent physical and chemical properties compared with the individual parts. Costantino et al. [7] have reported that the fluorescence emission of methyl orange (MO) molecule incorporated into Zn_2Al-LDH covers the whole visible wavelength range by changing the dye loading, owing to the different arrangement of the interlayer MO molecule. Wang et al. [8] has reported that tetra(8-hydroxyquinoline)boronate intercalated Mg_2Al-LDH showed a strong solid-state blue luminescence. It can be expected that the chromophore/LDH system cannot only improve the photophysical and photochemical properties of the guest, but also can increase their thermal- and photo-stability. Therefore, these studies confirm the LDH-based organic–inorganic hybrid materials exhibit interesting properties due to the suparmolecular interaction between host and guest materials.

8-Hydroxy-pyrene-1,3,6-trisulphonate (HPTS, as shown in Scheme 1) is a well-known water-soluble fluorescent molecule, which has been extensively used as a probe for a large number of scientific, medical and commercial applications due to its unique fluorescent properties (such as excellent photostability, high quantum yield, high absorbance, non-toxicity) [9–12]. It was reported that the photophysical properties of the pristine HPTS solution can be changed by adjusting its surrounding environment and the interaction fashion with other species [13,14]. For example, Ray and Nakahara have reported that the interaction of the HPTS dye with octadecylamine cation induce an obvious change in the emission spectrum of HPTS solution [15]. Roy et al. [16] have observed a slow excited state proton transfer (ESPT) from HPTS to acetate occur within the cetyltrimethyl ammonium bromide (CTAB) micellar medium because of a strong electrostatic interaction between the anionic probe HPTS with cationic surfactant CTAB. However, the tunable photophysical properties of the solid-state HPTS systems are still seldom to be reported, which largely restrict its application as solid-state luminescence and color display material.

* Corresponding author. Fax: +86 10 64425385.
E-mail address: lujun@mail.buct.edu.cn (J. Lu).

0022-4596/$ - see front matter © 2011 Elsevier Inc. All rights reserved.
doi:10.1016/j.jssc.2011.10.049

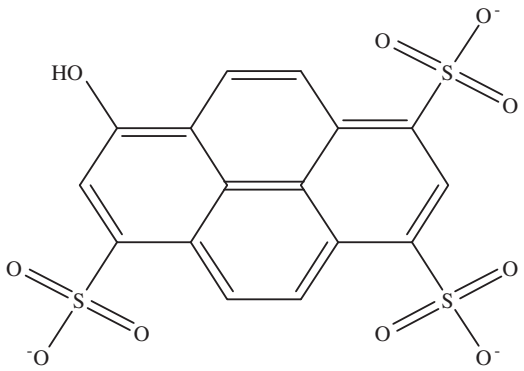

Scheme 1. Molecular structure of 8-hydroxypyrene-1,3,6-trisulphonate.

In the present work, HPTS and octanesulphonate (OS) anions have been employed to co-intercalate into the ZnAl-LDH layer by a hydrothermal co-precipitation method. New type of photofunctional materials, named as HPTS(x%)-OS/Zn_2Al LDHs, are constructed to study their luminescent properties dependent on the controllable interlayer microenvironments. In particular, an effort to investigate the co-intercalation effect and its possible application in adjustable solid-state luminescence was carried out. A series of samples with different contents of HPTS were prepared, and the photophysical properties of the resulting HPTS (x%)-OS/ZnAl LDH samples were investigated by steady-state and time-decay photoluminescence (PL) spectroscopy. The studies indicated that the emission of HPTS(x%)-OS/Zn_2Al-LDHs are strongly related to the guest aggregates and the interlayer guest–guest interaction. Among the HPTS(x%)-OS/Zn_2Al-LDH samples, it was obtained that the HPTS(2%)-OS/Zn_2Al-LDH exhibits the strongest blue luminescence and longest fluorescence lifetime. Moreover, the photoluminescent properties of chromophore–LDH hybrid materials can also be modulated by hydrothermal treatments at different pH. Thus, the tunable blue/green fluorescence emission can be obtained by changing the interlayer HPTS content, guest–guest and host–guest interaction, which paves a new way to develop new types HTPS-based solid dual-color luminescent materials.

2. Experiment

2.1. Materials

8-Hydroxy-pyrene-1,3,6-trisulphonic acid trisodium salt (Na_3HPTS, 85%) was purchased from Tokyo Chemical Industry Co. Ltd. Octanesulphonic acid sodium salt (NaOS, 98%) was purchased from J&K Chemical Co. Ltd. NaOH (AR), $Al(NO_3)_3 \cdot 9H_2O$ (AR), $Zn(NO_3)_2 \cdot 6H_2O$ (AR), C_2H_5OH (AR), and HNO_3 (AR) were purchased from the Beijing Chemical Co. Limited, and used without further purification. The carbonate-free deionized water was used throughout the experimental processes.

2.2. Synthesis of HPTS(x%)-OS/Zn_2Al LDH

The co-intercalated HPTS(x%)-OS/Zn_2Al LDHs were prepared by a hydrothermal co-precipitation method as follows: $Zn(NO_3)_2 \cdot 6H_2O$ (4.46 g, 15 mmol), $Al(NO_3)_3 \cdot 9H_2O$ (2.84 g, 7.5 mmol), NaOS (a mmol) and Na_3HPTS (b mmol, $a+3b=7.5$) were dissolved in a mixed solvent of water and ethanol (30% ethanol by volume) 50 mL with the pH value adjusted to 5.5 by slowly adding NaOH (0.5 M) solution under N_2 atmosphere to prevent contamination of CO_2. The value x% stands for the initial molar percentage of HPTS in HPTS and OS ($x\% = b/(a+b) \times 100\%$; x% = 1%, 2%, 5%, 10%, 20%, and 100% were employed). The solution mixture was aged in an autoclave at 80 °C for 24 h.

2.3. Fabrication of HPTS-OS/ZnAl LDH films

Films of HPTS-OS/ZnAl LDH were prepared by the solvent evaporation method: the hydrothermally aged product was washed thoroughly without drying and then a suspension prepared by adding ethanol (0.1 g/50 mL). The suspension of HPTS-OS/ZnAl LDH was then thoroughly ultrasonically dispersed and spread on a glass substrate (which was ultrasonically cleaned in distilled water and anhydrous ethanol several times), and then dried in vacuum at ambient temperature for 5 h.

2.4. Characterization

The XRD measurements were performed on a Rigaku XRD-6000 diffractometer, using Cu-$K\alpha$ radiation ($\lambda = 0.15418$ nm) at 40 kV, 30 mA, with a scanning rate of $10^\circ min^{-1}$, and a 2θ angle ranging from 3° to 70°. Elemental analysis (Al, Zn, S) was performed by atomic emission spectroscopy with a Shimadzu ICPS-7500 instrument. C, H, and N contents were determined using a Perkin Elmer Elementarvario elemental analysis instrument. Scanning electron microscope (SEM) images were obtained using a Hitachi S-4700 scanning electron microscope operating at 20 kV. The UV–vis absorption spectra were recorded on a Shimadzu U-3000 spectrophotometer in the range from 250 to 600 nm with a slit width of 1.0 nm, and $BaSO_4$ was used as reference. The fluorescence spectra were performed on an Hitachi F-7000 FL spectrophotometer with a slit width of 5 nm, excitation at 375 nm, emission spectra of 400–600 nm, and a PMT voltage of 400 V. Fluorescent lifetime measurements were recorded with an Edinburgh Instruments FL 900 fluorimeter. The percentage contribution of each lifetime component to the total decay was calculated with the Edinburgh F900 instruments software.

3. Results and discussion

3.1. Structural and compositional characterization of HPTS(x%)-OS/ZnAl LDH

The XRD patterns of HPTS(x%)-OS/ZnAl LDH powder samples are shown in Fig. 1. In each case, the XRD pattern exhibits the characteristic reflections of the LDH layered structure with a series of *00l* peaks with narrow, strong lines at low angle indicating organic macromolecules has been assembled into the interlayer. The *00l* peaks do not appear in rigorous symmetric, which may be attributed to the disorder and slippage of the basal plane in pillared clays [17,18]. The interlayer spacing can be calculated from averaging the positions of the three harmonics: $c = (1/3)\ (d_{003} + 2d_{006} + 3d_{009})$. For the HPTS(1%)-OS/$Zn_2Al$ LDH sample, the 003 reflection (Fig. 1, curve a) appears at $2\theta = 4.06^\circ$ with an interlayer distance of 2.11 nm. Furthermore, for other co-intercalation samples, the 003 reflection appear at 4.18°, 3.93°, 4.07° and 4.02° for HPTS(x%)-OS/Zn_2Al LDH, where $x = 2$, 5, 10, and 20, respectively. The variation of the interlayer spacing can be assigned to variable arrangements of interlayer guest molecules with different ratios of HPTS to OS and tunable host–guest and guest–guest interaction [7,19]. The gallery height of co-intercalation samples thus can be estimated in the range 1.62–1.76 nm upon exclusion of the thickness of the host layer (0.48 nm), indicating OS anions (the anion size: *ca.* 1.04 nm) show a tilted bilayer arrangement with respective to the LDH layer. The 003 reflection of pure HPTS/Zn_2Al LDH (Fig. 1, curve f) appears at

$2\theta = 5.99^{\circ}$ (gallery height of 1.00 nm), which is consistent well with the anion size (ca. 1.01 nm for HPTS). That is, the long-axis of the HPTS anions is approximately perpendicular to the brucite-like layers. The lattice parameter a, which stands for the shortest distance of adjacent metal atoms with identical chemical environment in the LDH layer, can also be calculated by $a = 2d_{110}$. The values of a for these samples are in the range 3.03–3.05 Å, in accordance with other reported LDH system. Therefore, based on the charge conservation between the interlayer anion and the cationic layer, it can be estimated that the average interplanar distance between the interlayer anion is approximately 5.28 Å in the case of low concentration of HTPS. The chemical compositions of the resulting products are listed in Table 1. It can be seen that the ratios of divalent to trivalent metals are in the range 1.90–2.55, which is close to those in the corresponding synthesis mixture for HPTS(x%)-OS/Zn_2Al LDH, indicating that both divalent and trivalent metals are quantitatively precipitated during the co-precipitation process. The observed HPTS content (x%) is close to the initial nominal content, and the increased trend is consistent with the increasing initial HPTS concentration throughout the whole concentration range, as expected among the HPTS(x%)-OS/Zn_2Al LDH samples.

3.2. Optical properties of HPTS(x%)–OS/Zn_2Al-LDH

3.2.1. Optimal luminous intensity and lifetime

In the aqueous solution, HPTS molecule shows a weak emission band at 440 nm and a stronger band at 510 nm, which correspond to the protonated form (ROH) and deprotonated form (RO^-) of HPTS, respectively [20]. The fluorescent emission spectra for HPTS-OS/Zn_2Al-LDH with different content of HPTS are shown in Fig. 2. The optimal luminous intensity presents in the HPTS(2%)-OS/LDH sample, which shows a dual fluorescence with the peak at 437 nm (blue emission) and 515 nm (green emission). This phenomenon is consistent with that of the aqueous solution, indicating that the chromophore–chromophore interactions and aggregation does not form under low HPTS content within the LDH layer. For the HPTS(1%)-OS/LDH sample, the reduction of the fluorescence intensity can be attributed to the lower content of HPTS fluorescent molecules. Upon increasing concentration of HPTS with x% from 2% to 20%, the fluorescence intensity decreases rapidly due to the formation of aggregation. The similar behavior has been described in previous studies [21,22]. The fluorescent spectra clearly confirm that the introduction of OS in the gallery of LDH can enhance the emission intensity significantly compared with the pure HPTS powder (Fig. 2, curve f). Ogawa and Kuroda [23] reported that surfactants can alter the aggregation of photoactive species. In our opinion, the intercalated long-chain surfactants can homogenously dilute and isolate the interlayer HPTS molecules, and thus the distance between dye molecules is enlarged enough for preventing the formation of aggregates. Another advantage of the surfactant molecules is that they can pre-intercalate the LDH layers for enlarging the interlayer spacing, which is benefit to the intercalation of bulky dye molecules [24]. It should be noted that it is important to find the optimal luminous condition for the dye and surfactant cointercalated layered matrix in actual application, not only for saving the cost of dye, but for the maximization of the luminescence efficiency. Moreover, as we have known, the dual-color fluorescent emission from a solid-state material are seldom observed compared with those of the solution system [25]. For the HPTS(x%)-OS/LDH sample, the dual-color fluorescence between the blue and green regions can also be controlled by changing the interlayer HPTS content, i.e., the ratio of the intensity between the blue (437 nm) and green (515 nm) fluorescence increase firstly from 0.44

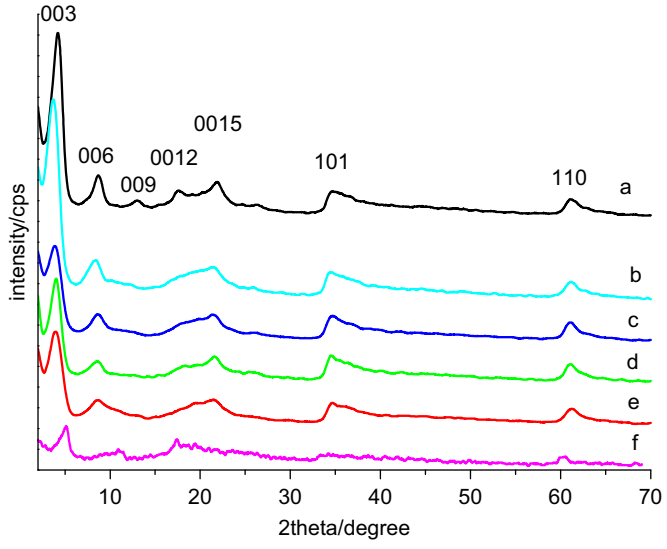

Fig. 1. XRD patterns of the HPTS-OS/LDH film.

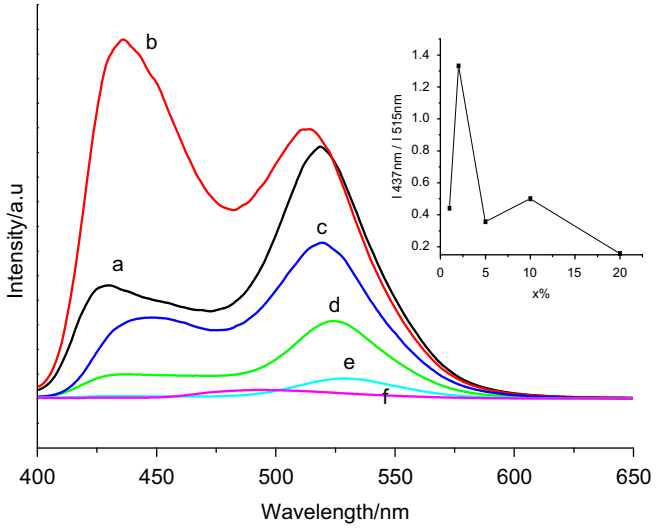

Fig. 2. Photoluminescence spectra of HPTS(x%)-OS/LDH: (a)–(e) x%=1%, 2%, 5%, 10%, 20% and (f) pure HPTS powder.

Table 1
Chemical compositions of the resulting products.

x%	Chemical composition	Zn/Al ration	Experimental content x%
1	$Zn_{0.706}Al_{0.294}(OH)_2(OS)_{0.264}(HPTS)_{0.00156}(CO_3)_{0.00514}(NO_3)_{0.0150} \cdot 0.89H_2O$	2.40	1.76
2	$Zn_{0.655}Al_{0.345}(OH)_2(OS)_{0.247}(HPTS)_{0.00362}(CO_3)_{0.0139}(NO_3)_{0.0591} \cdot 0.74H_2O$	1.90	3.15
5	$Zn_{0.668}Al_{0.332}(OH)_2(OS)_{0.231}(HPTS)_{0.00635}(CO_3)_{0.0176}(NO_3)_{0.0468} \cdot 1.24H_2O$	2.01	7.63
10	$Zn_{0.696}Al_{0.304}(OH)_2(OS)_{0.201}(HPTS)_{0.0102}(CO_3)_{0.0117}(NO_3)_{0.0490} \cdot 1.08H_2O$	2.29	13.26
20	$Zn_{0.718}Al_{0.282}(OH)_2(OS)_{0.166}(HPTS)_{0.0181}(CO_3)_{0.0119}(NO_3)_{0.0380} \cdot 0.94H_2O$	2.55	24.72

($x\%=1\%$) to 1.33 ($x\%=2\%$) and then further decrease to 0.16 ($x\%=20\%$), suggesting these organic–inorganic solid samples have potential application in the field of tunable solid luminescent materials.

To understand the excited state information of the samples, the HPTS($x\%$)-OS/LDH were further studied by detecting their fluorescence decays, with excitation and emission wavelength of 360 and 440 nm, respectively. The fluorescence lifetimes were obtained by fitting the decay profiles with double-exponential forms, and results are tabulated in Table 2. The average lifetime $<\tau>$ is also listed.

The HPTS($x\%$)-OS/LDH powder samples exhibit tunable fluorescence lifetime from 0.61 to 3.08 ns with $x\%$ value in the range 1–20%. The fluorescence lifetime increases at first to a maximum (2%: 3.08 ns), and then decreases as the increase of the ratio of HTPS to OS. This trend is consistent well with that of the fluorescence intensity, which can be attributed to the formation of aggregates in the high content HTPS samples.

Table 2
Fluorescence lifetimes of the resulting products.

Samples ($x\%$)	τ_1	A_1 (%)	τ_2	A_2 (%)	$\langle\tau\rangle$	χ^2
1	1.181	12.39	3.250	87.61	2.994	1.302
2	1.824	21.40	3.419	78.60	3.078	1.136
5	1.226	32.75	2.797	67.25	2.282	1.151
10	0.7871	45.09	2.211	54.91	1.569	1.249
20	0.3559	79.04	1.561	20.96	0.6085	1.288

τ_1 and τ_2 correspond to two lifetimes; A_i stands for the percentage of τ_i. The goodness of fit is indicated by the value of χ^2. In the double-exponential case, $\langle\tau\rangle=A_1\tau_1+A_2\tau_2$; $A_1+A_2=1$.

3.2.2. *Shielding effect of the LDH from Cu^{2+} quencher*

Biswas et al. [26] reported that Cu^{2+} is a efficient quencher cation for HPTS solution. Fig. S1 in Supporting Information shows that the fluorescent intensity of dye decrease as the increasing quencher concentration in bulk aqueous environment; under high Cu^{2+} concentration (10^{-1} mol/L), the emission peak of the HPTS solution almost disappears. In this section, we mainly study whether the similar quenching behavior can appear for the solid-state HPTS-OS/Zn_2Al-LDH film sample, because it is important to understand the different luminescent properties between solid and solution systems.

HPTS(2%)-OS/LDH film was fabricated using the solvent evaporation method. The XRD pattern for HPTS(2%)-OS/LDH film prepared by the solvent evaporation method show a strong 003 reflection implying good crystallinity of film (Fig. 3). Fig. 4 displays the SEM images of the HPTS(2%)-OS/Zn_2Al-LDH, which exhibit a smooth and continuous surface in the top view. The individual platelets are densely packed with ab-plane parallel to the substrate. The thickness of the film is estimated ca. 200 nm by observing the side view of the film.

Fig. 5 shows the fluorescent spectra of HPTS(2%)-OS/Zn_2Al-LDH film sample under different Cu^{2+} concentration, which shows that the fluorescent intensity is nearly unchanged upon immersing into the solution different Cu^{2+} concentration. This phenomenon illustrates that the HPTS assembled LDH film is insensitive upon increasing quencher concentration. This insensitivity of quencher

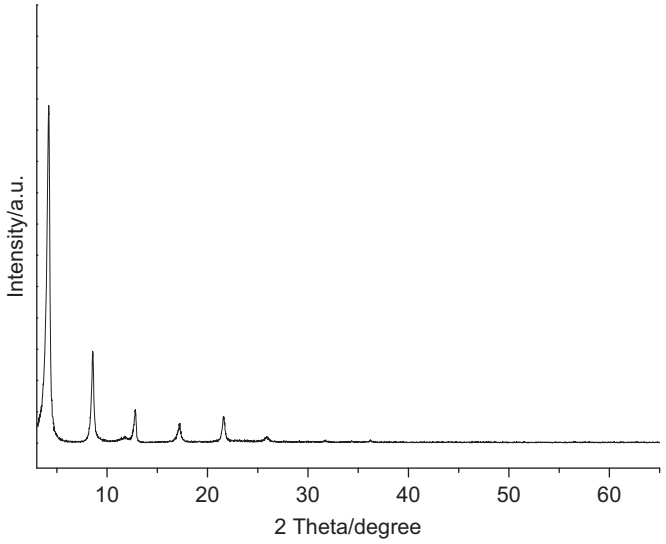

Fig. 3. XRD patterns of the HPTS-OS/LDH film.

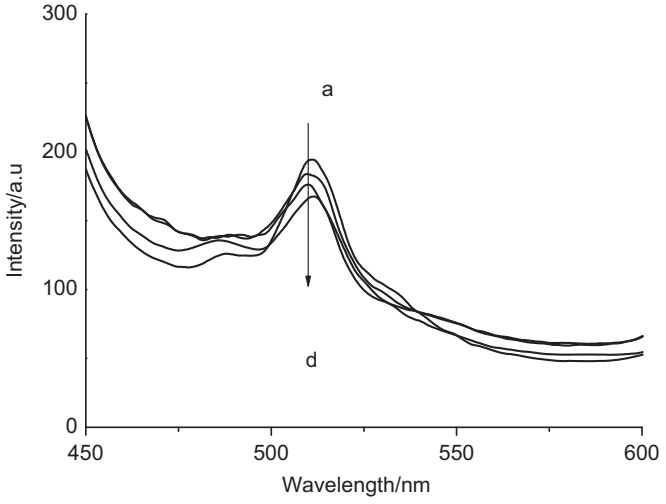

Fig. 5. Photoluminescence spectra of HPTS-OS/LDH film in various Cu^{2+} concentrations solution: (a) 10^{-4} mol/L, (b)10^{-3} mol/L, (c) 10^{-2} mol/L and (d)10^{-1} mol/L.

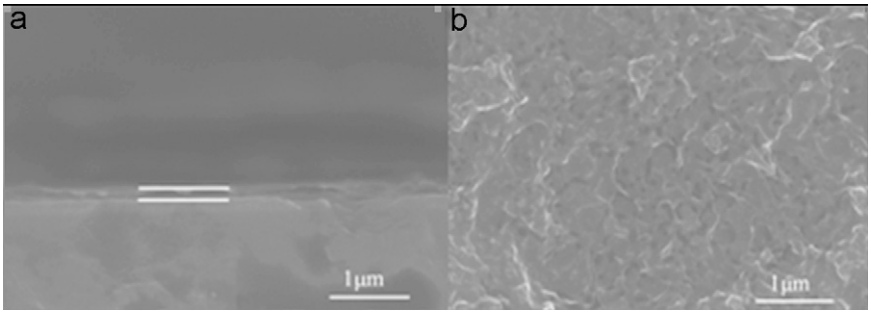

Fig. 4. SEM images of HPTS(2%)-OS/LDH film: (a) side view image and (b) top view image.

concentration in solution further confirms that HPTS molecules are not adsorbed on the interface of LDH but intercalated into the gallery of LDH. The LDH host layer shield the interlayer HPTS from Cu^{2+} quencher with positive charges. The repulsive force between LDH layer and positive charges in solution prevent the contact of Cu^{2+} and the dye, which hinder the quenching process and thus enhance the luminescence efficiency. Another factor is that the confinement effect of LDH restrict the rotation and vibration of species in the gallery and hinder the quenching process depended on the collision.

3.2.3. *Comparison studies on fluorescence under different microenvironment*

It was well documented that the luminescence property of HPTS is strongly related to the pH value. For example, in alkaline medium, pH > 7.4, the deprotonated form (RO^-) of the dye are preferred due to the acid–base equilibrium. The electronic structures of RO^- is unchanged during the photoexcitation process, which corresponds to a singlet excitation [27,28]. Fluorescence at this state undergoes a fast Stokes shift (0.4 ps) and has a maximum value at 510 nm and a lifetime of 5.3 ± 0.1 ns [28,29]. In acidic medium, pH < 7.4, the conjugate acid form (ROH) dominates in the ground state. Fluorescence at this state undergoes a fast Stokes shift (0.3 ps) and has a maximum value near 440 nm. Excited state proton transfer (ESPT) takes place in 87.5 ps [27–29] to yield the conjugate base (RO^-), with a fluorescence maximum at 515 nm and a lifetime of 4.8 ± 0.5 ns. Therefore, in both acidic and basic aqueous environments of HPTS solution, the emission spectrum is nearly unchanged and the blue emission bands are difficult to observe.

The fluorescence spectra of HPTS in aqueous media and in the gallery of Zn_2Al-LDH have been shown in Fig. 6. To avoid the influence of pH value on the emission, we disperse the HPTS and HPTS(2%)-OS/Zn_2Al-LDH powders into water (pH=5.5) to form solution and colloid, respectively. It can be observed that the emission intensity at 440 nm of HPTS(2%)-OS/Zn_2Al-LDH colloid is significantly higher than that of HPTS solution under pH=5.5. For HPTS(2%)-OS/Zn_2Al-LDH colloid, the ROH band intensity at 440 nm is stronger than that of the RO^- band at 510 nm. The emission spectra reveals that the amount of ROH^* in the excited states is larger than its solution counterpart [30–32]. Therefore, the luminescence property of HPTS in the LDH gallery is significantly different from that in the aqueous media. This can be attributed to the inhibition of ESPT process by LDH host. In an unique microenvironment of LDH gallery, HPTS molecules are surrounded by LDH layer with positive charges, and the deprotonation become difficult, which lead to the enhancement of blue emission. On the other hand, a rigid and confined environment of the host makes configuration difficult to transfer between protonated and deprotonated forms than that in aqueous media.

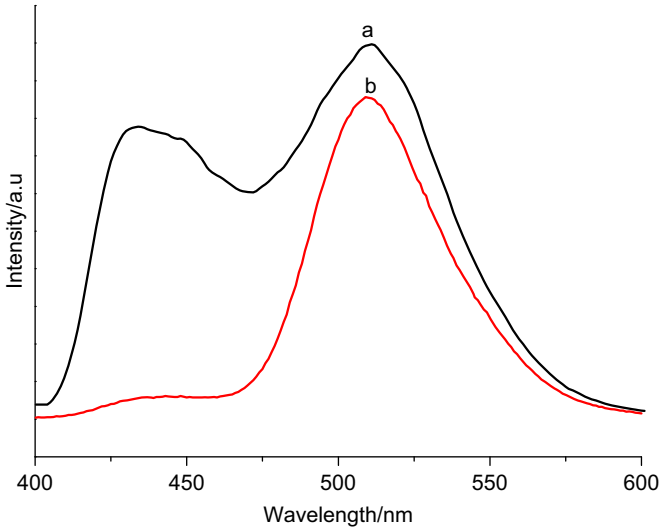

Fig. 6. Photoemission spectra: (a) HPTS(2%)-OS/LDH and (b) HPTS solution, both at pH=5.

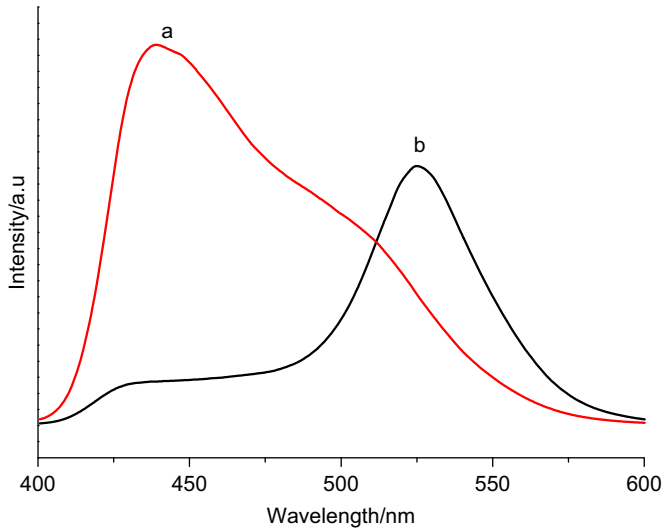

Fig. 7. Controllability of fluorescence emission: (a) samples after hydrothermal treatments 6 h at acidic media and (b) samples after hydrothermal treatments 6 h at neutral media.

3.3. *Controllable luminescent properties*

According to the result above, the HPTS(2%)-OS/Zn_2Al-LDH was chosen as a model system to investigate its controllable luminescent properties under different pH media. After the powder was further treated under hydrothermal conditions at neutral (pH=7, sample A) and acidic (pH=4, sample B) media for 6 h, respectively, a significant change was observed. Sample B emits a bright blue luminescence while a strong green luminescence was observed in Sample A (Fig. 7). It has been known that absorption spectra and fluorescence of pure HPTS solution is solvent-dependent [33,34]. In aqueous media, the absorption spectra of ROH and RO^- species were at 405 and 450 nm, respectively, [34]. Therefore, the absorption spectra can also reveal the HPTS state (ROH or RO^-) in the gallery of LDH. Fig. 8 show that sample A has a strong absorption at 450 nm due to the RO^- form in the LDH layer, while sample B has a strong absorption around 405 nm, which belong to the ROH form. Thus, it can be concluded that states of the HPTS in the gallery of LDH can transfer between two forms by changing different hydrothermal conditions, which can further control the luminescent properties of the hybrid materials.

4. Conclusion

In summary, HPTS and OS anions were selected to co-intercalate into Zn_2Al-LDH by the hydrothermal co-precipitation method, and the HPTS-OS/LDH film was fabricated by solvent evaporation method. For HPTS(x%)-OS/Zn_2Al LDH systems, the fluorescence wavelength and intensity of the intercalated HPTS correlate strongly with the interlayer microenvironment and intermolecular interaction of HPTS within the LDH gallery. The optimal luminous intensity and longest fluorescence lifetime present in HPTS(2%)-OS/Zn_2Al LDH. The emission intensity at 440 nm of HPTS(2%)-OS/Zn_2Al-LDH colloid is significantly higher

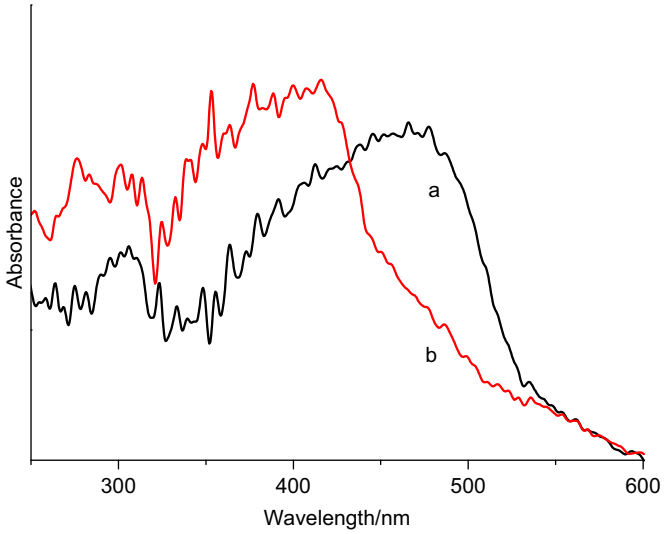

Fig. 8. UV–vis absorption spectra of HPTS(2%)-OS/LDH powder: (a) samples after hydrothermal treatments 6 h at neutral media and (b) samples after hydrothermal treatments 6 h at acidic media.

than that of HPTS solution under pH=5.5, suggesting that the LDH layer can hinder ESPT effectively and induce a significant change in the luminescent properties. Furthermore, this work provides a facile approach to modulate the photoluminescent properties of chromophore–LDH hybrid materials by simply hydrothermal treatments under different pH. Therefore, the controllable sates of the HPTS within the LDH layer supplies opportunities for the design and application of LDH-based chromophores in the field of solid luminescent materials.

Acknowledgments

This work was supported by the National Natural Science Foundation of China, the 111 Project (Grant no. B07004), the Fundamental Research Funds for the Central Universities, and the 973 Program (Grant no. 2011CBA00504).

Appendix A. Supplementary materials

Supplementary materials associated with this article can be found in the online version at doi:10.1016/j.jssc.2011.10.049.

References

[1] V. Prevot, C. Forano, J.P. Besse, Inorg. Chem. 37 (1998) 4293–4301.
[2] B. Johann, B. Peter, S. Markus, L. Heinz, Adv. Funct. Mater. 13 (2003) 241–248.
[3] L. Ukrainczyk, M. Chibwe, T.J. Pinnavaia, S.A. Boyd, J. Phys. Chem. 98 (1994) 2668–2676.
[4] T. Saito, J.I. Kadokawa, H. Tagaya, Trans. Mater. Res. Soc. Jpn. 26 (2001) 503–509.
[5] D.P. Yan, J. Lu, M. Wei, S. Qin, L. Chen, S. Zhang, D.G. Evans, X. Duan, Adv. Funct. Mater. 21 (2011) 2497–2505.
[6] D.P. Yan, J. Lu, J. Ma, S. Qin, M. Wei, D.G. Evans, X. Duan, Angew. Chem. Int. Ed. 50 (2011) 7037–7040.
[7] U. Costantino, N. Coletti, M. Nocchetti, G.G. Aloisi, F. Elisei, Langmuir 15 (1999) 4454–4460.
[8] Z.L. Wang, Z.H. Kang, E.B. Wang, Z.M. Su, L. Xu, Inorg. Chem. 45 (2006) 4364–4371.
[9] S. Pramanik, P. Banerjee, S.C. Bhattacharya, J. Photochem. Photobiol. A: Chem. 187 (2007) 384–388.
[10] R.B. Rodriguez, J. Estelrich, J. Photochem. Photobiol. A: Chem. 198 (2008) 262–267.
[11] C.R. Zamarreno, J. Bravo, J. Goicoechea, I.R. Matias, F.J. Arregui, Sensors Actuators B 128 (2007) 138–144.
[12] R.B. Rodriguez, J. Estelrich, J. Phys. Chem. B 113 (2009) 1972–1981.
[13] J.R. Lakowicz, Principles of Fluorescence Spectroscopy, 3rd Edition, Springer, 2006.
[14] P.K. Dutta, D.S. Robbins, Langmuir 10 (1994) 4681–4687.
[15] K. Ray, H. Nakahara, J. Photochem. Photobiol. A: Chem. 173 (2005) 75–80.
[16] D. Roy, R. Karmakar, S.K. Mondal, K. Sahu, K. Bhattacharyya, Chem. Phys. Lett. 399 (2004) 147–151.
[17] G.S. Thomas, V. Kamath, S. Kannan, J. Phys. Chem. C 111 (2007) 18980–18984.
[18] S.V. Prasanna, P. Vishnu Kamath, C. Shivakumara, J. Colloid Interf. Sci. 344 (2010) 508–512.
[19] D.P. Yan, J. Lu, J. Ma, M. Wei, S. Qin, L. Chen, D.G. Evans, X. Duan, J. Mater. Chem. 20 (2010) 5016–5024.
[20] P. Leiderman, R. Gepshtein, A. Uritski, L. Genosar, D. Huppert, J. Phys. Chem. A 110 (2006) 5574–5581.
[21] D.P. Yan, J. Lu, M. Wei, D.G. Evans, X. Duan, J. Phys. Chem. B 113 (2009) 1381–1388.
[22] S.D. Li, J. Lu, J. Xu, S.L. Dang, D.G. Evans, X. Duan, J. Mater. Chem. 20 (2010) 9718–9725.
[23] M. Ogawa, K. Kuroda, Chem. Rev. 95 (1995) 399–438.
[24] L. Mohanambe, S.J. Vasudevan, J. Phys. Chem. B 110 (2006) 14345–14354.
[25] N. Chandrasekharan, L.A. Kelly, J. Am. Chem. Soc. 123 (2001) 9898–9899.
[26] S. Biswas, S.C. Bhattacharya, S.P. Moulik, J. Colloid Interf. Sci. 271 (2004) 157–162.
[27] T.H. Tran-Thi, T. Gustavvson, C. Prayer, S. Pommeret, J.T. Hynes, Chem. Phys. Lett. 329 (2000) 421–430.
[28] J.M. Dela Cruz, I. Pastirk, V.V. Lozovoy, K.A. Walowicz, M. Dantus, J. Phys. Chem. A 108 (2004) 53–58.
[29] T.H. Tran-Thi, C. Prayer, P.H. Millie, P. Uznanski, J.T. Hynes, Phys. Chem. A 106 (2002) 2244–2255.
[30] S. Pramanik, P. Banerjee, S.C. Bhattacharya., J. Photochem. Photobiol. A: Chem. 187 (2007) 384–388.
[31] S. Gago, T. Costa, J.S. de Melo, I.S. Goncalves, M. Pillinger, J. Mater. Chem. 18 (2008) 894–904.
[32] E. Pines, D. Huppert, N.J. Agmon, Chem. Phys. 88 (1988) 5620–5630.
[33] M. Rini, B.Z. Magnes, E. Pines, E.T.J. Nibbering, Science 301 (2003) 349–352.
[34] P. Leiderman, R. Gepshtein, A. Uritski, L. Genosar, D. Huppert, J. Phys. Chem. A 110 (2006) 5573–5584.